Supplementary Material

Performance and Mechanisms of Cd(II) Removal by Phosphate-Modified Natural Pyrite

Lili Lin[c, 1], Chao Wang[a, 1], Xiaoshan Luo[c], Ziwei Tai[a], Yaxin Qin[a, *], Wei Liu[b, *]

[a]School of Chemistry and Environmental Engineering, Wuhan Institute of Technology, Wuhan 430205, People's Republic of China

[b]State Key Laboratory of Green and Efficient Development of Phosphorus Resources, Hubei Key Laboratory of Novel Reactor and Green Chemical Technology, School of Chemical Engineering and Pharmacy, Wuhan Institute of Technology, Wuhan 430205, People's Republic of China

[c]Central-Southern China Environmental Test and Detection Technology Institute (Wuhan) Co., Ltd.

[1]These authors should be considered co-first authors.

*To whom correspondence should be addressed. E-mail: qinyaxin168@163.com (Y. Qin); liu_wei@wit.edu.cn (W. Liu).

Text S1. Chemicals

The natural pyrite (FeS_2) was sourced from Wuhan Wanquan Mining Co., Ltd. Hydrochloric acid (HCl), nitric acid (HNO_3), potassium dihydrogen phosphate (KH_2PO_4), cadmium nitrate ($Cd(NO_3)_2 \cdot 4H_2O$), ascorbic acid ($C_6H_8O_6$), ammonium molybdate tetrahydrate ($H_{32}Mo_7N_6O_{28}$), potassium antimony tartrate ($C_8H_8KO_{12}Sb$), and anhydrous ethanol (CH_3CH_2OH) were purchased from Shanghai Sinopharm Chemical Reagent Co., Ltd. Humic acid (HA) and fulvic acid (FA) were obtained from Shanghai Yuanye Biotechnology Co., Ltd. All chemical reagents were analytical pure and used without further purification. Ultrapure water (> 18 MΩ•cm, PGDZ-10-XH, Pinguan, China) was utilized in all experiments.

Text S2. Characterizations

Powder X-ray diffraction patterns (XRD) of FeS_2^{bm} and $FeS_2@P^{bm}$ were characterized using a Bruker D8 Advance X-ray diffractometer with Cu Kα radiation (λ = 0.15418 nm). Scanning electron microscope with energy dispersive X-ray (SEM-EDX, Regulus8100, Hitachi, Japan) was utilized to determine the surface feature and element contents of FeS_2^{bm} and $FeS_2@P^{bm}$. The content of phosphorus modified on $FeS_2@P^{bm}$ was determined by inductively coupled plasma-atomic emission spectroscopy (ICP-AES). The Zeta potential of FeS_2^{bm} and $FeS_2@P^{bm}$ were determined using a Zeta potential analyzer (Malvern Zen3600, UK). Chemical states of surface constituents were recorded by Fourier Transform Infrared Spectroscopy (FT-IR, Nicolet iS50, USA), Raman spectrometer (Raman, Thermo DXR Microscope, USA), and XPS (Thermo Scientific K-Alpha, US).

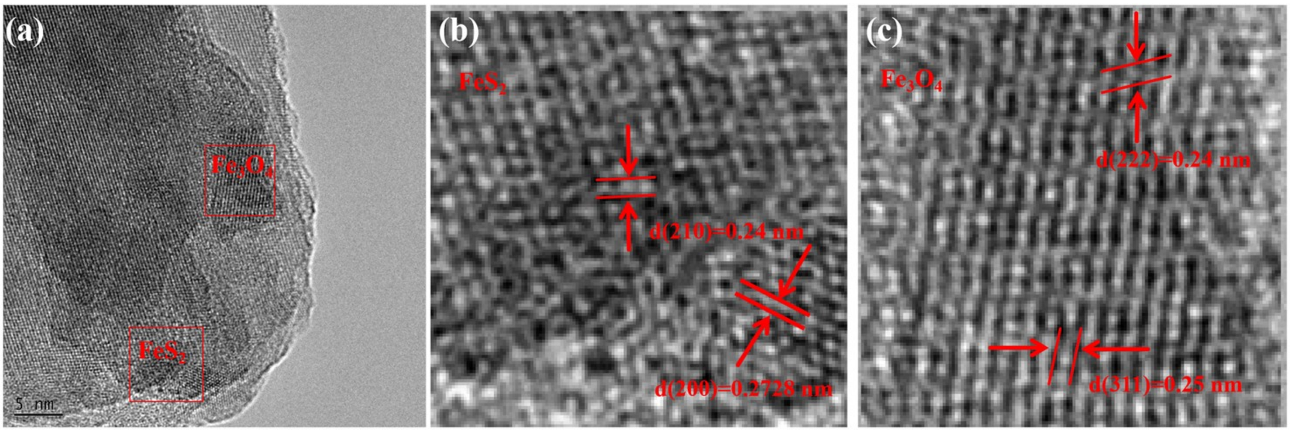

Fig. S1. TEM images of FeS_2@P^{bm}.

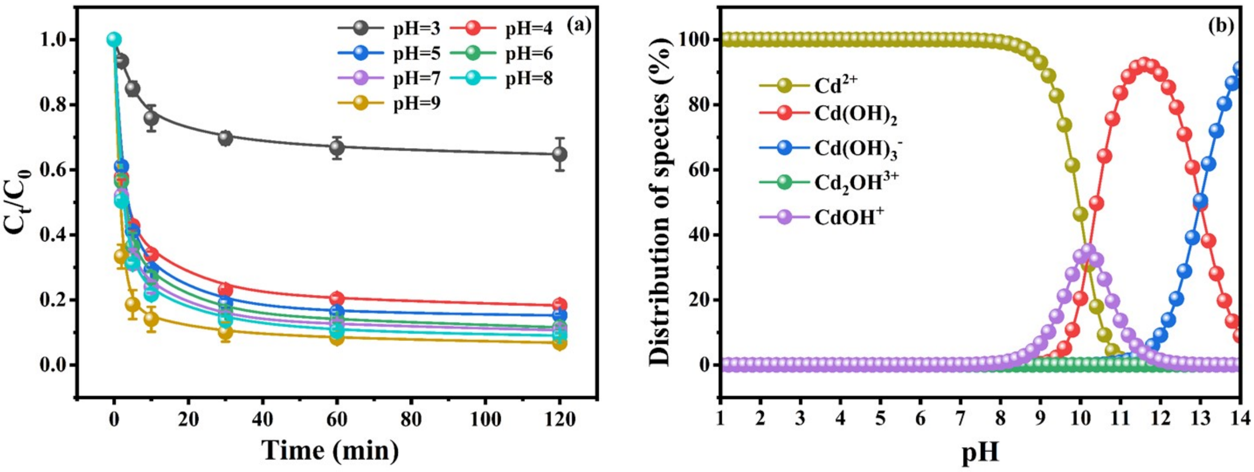

Fig. S2. (a) Effects of pH on Cd(II) removal efficiency by $FeS_2@P^{bm}$; (b) theoretical calculation of Cd(II) species distribution at different pH values. $[Cd(II)]_0$ = 30 mg/L and $[FeS_2@P^{bm}]_0$ = 0.6 g/L.

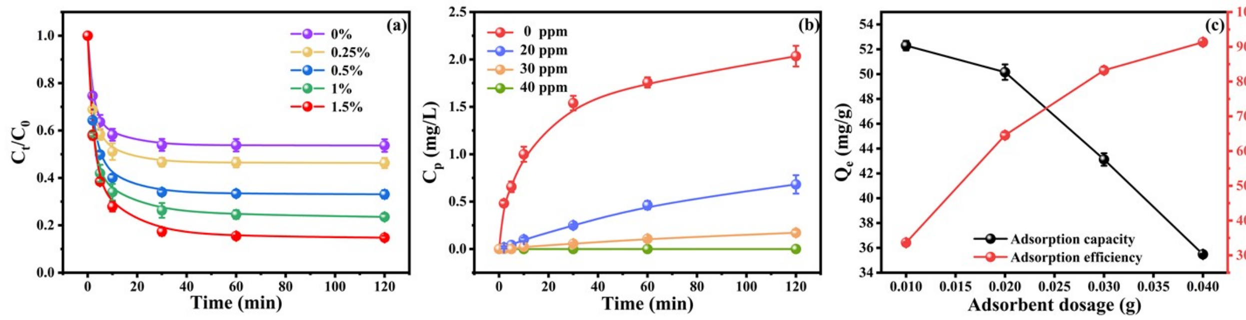

Fig. S3. Effects of phosphorus modification ratios on the removal of Cd(II); (b) the released concentration of phosphorus from $FeS_2@P^{bm}$ with different Cd(II) concentrations. (c) effects of adsorbent dosages on the adsorption efficiency of Cd(II) by $FeS_2@P^{bm}$. $[Cd(II)]_0$ = 30 mg/L, $[FeS_2@P^{bm}]_0$ = 0.6 g/L, and $pH_{initial}$ = 5.8.

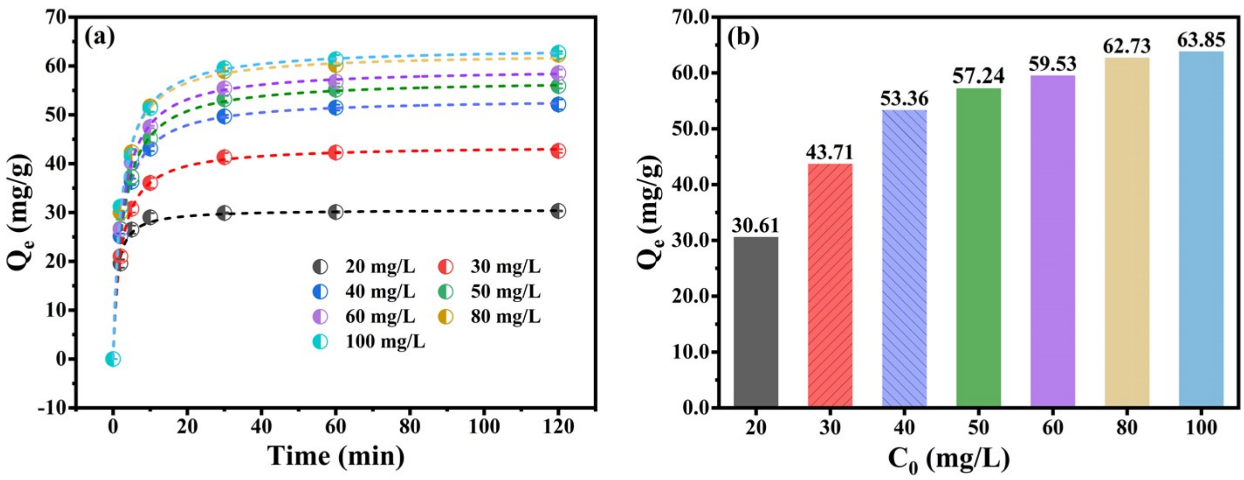

Fig. S4. (a) Pseudo-second-order kinetic plots,and pseudo-second-order kinetic rate constants (*k*) of of Cd(II) on $FeS_2@P^{bm}$ at different initial Cd(II) concentrations. $[FeS_2@P^{bm}]_0$ = 0.6 g/L and $pH_{initial}$ = 5.8.

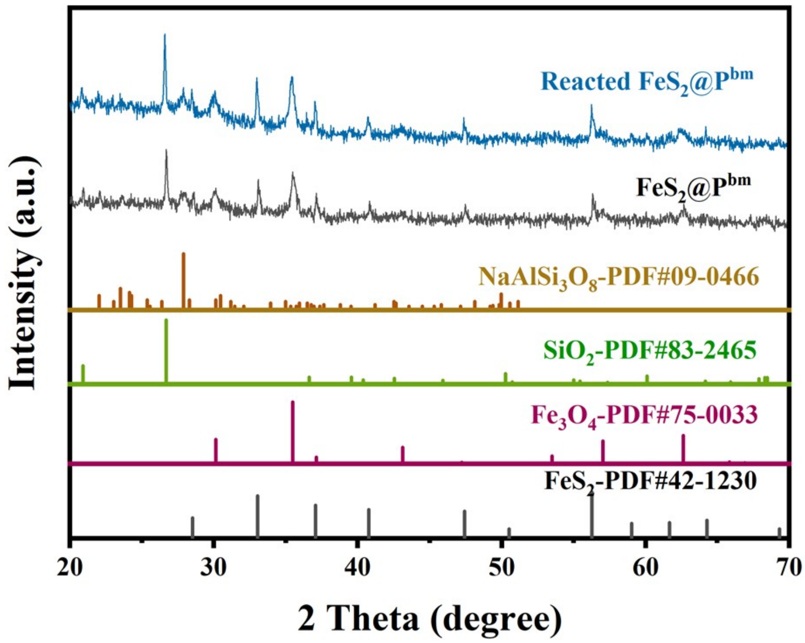

Fig. S5. XRD patterns of pristine and reacted FeS_2@P^{bm}.

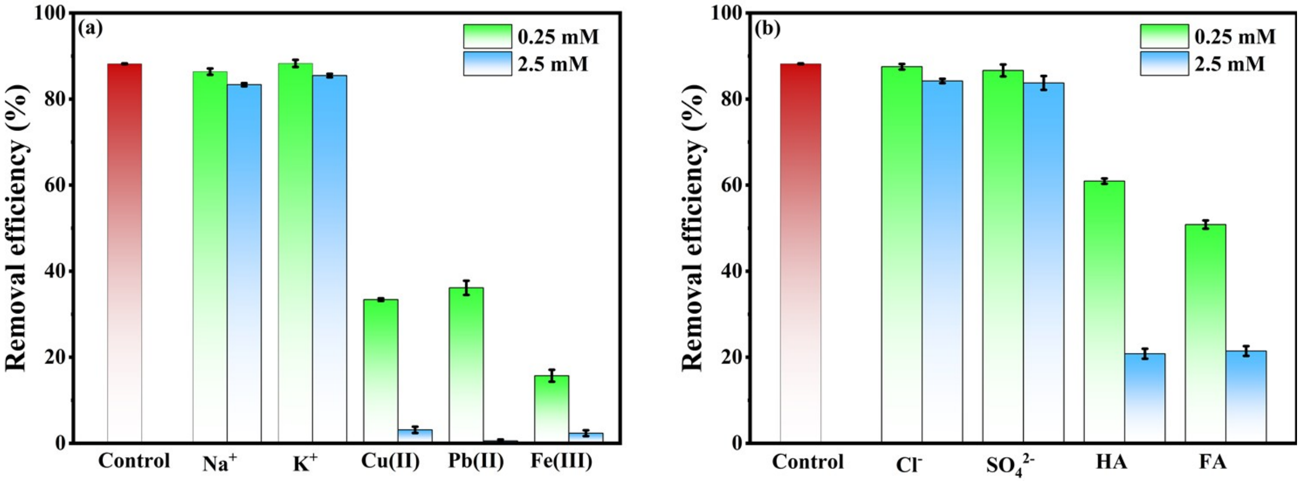

Fig. S6. Effects of coexisting ions and natural organic matter on the adsorption efficiency of Cd(II) by $FeS_2@P^{bm}$. $[Cd(II)]_0$ = 30 mg/L, $[FeS_2@P^{bm}]_0$ = 0.6 g/L, and $pH_{initial}$ = 5.8.

Table S1. BET surface area, total pore volume, and average pore diameter of FeS_2^{bm} and $FeS_2@P^{bm}$.

Samples	Surface area/($m^2 \cdot g^{-1}$)	Total pore volume/($cm^3 \cdot g^{-1}$)	Average pore diameter/(nm)
FeS_2^{bm}	35.61	0.057	6.89
$FeS_2@P^{bm}$	12.32	0.052	16.63

Table S2. Fitting parameters for pseudo-first-order and pseudo-second-order models that describe Cd(II) adsorption on FeS_2^{bm} and $FeS_2@P^{bm}$.

Model	Parameter	Material	
		FeS_2^{bm} (0%)	$FeS_2@P^{bm}$ (1.5%)
Pseudo-first-order	Q_e^a (mg•g^{-1})	23.16	42.60
	Q_e^b (mg•g^{-1})	22.67	41.19
	k_1 (min^{-1})	0.36	0.30
	R^2	0.9903	0.9833
Pseudo-second-order	Q_e^b (mg•g^{-1})	23.93	43.77
	K_2 (min^{-1})	0.03	0.01
	R^2	0.9981	0.9997

Table S3. Fitting parameters for the pseudo-second-order model that describe different initial concentrations Cd(II) adsorption on $FeS_2@P^{bm}$.

Model	Pseudo-second-order model						
C_0 (mg•L^{-1})	20	30	40	50	60	80	100
Q_t (mg•g^{-1})	30.31	42.60	52.12	55.88	58.51	62.29	62.70
Q_e^b (mg•g^{-1})	30.61	43.71	53.36	57.24	59.53	62.73	63.85
K_2 (min^{-1})	0.035	0.011	0.008	0.006	0.006	0.007	0.007
R^2	0.9999	0.9999	0.9999	0.9999	0.9999	0.9999	0.9999

Table S4. Fitting parameters for the pseudo-first-order and pseudo-second-order models that describe Cd(II) adsorption on FeS_2@P^{bm} under different temperatures.

Model	Parameter	Temperature/K		
		298	308	318
Pseudo-first-order	Q_e^a ($mg•g^{-1}$)	44.67	46.68	47.24
	Q_e^b ($mg•g^{-1}$)	42.68	44.62	45.29
	k_1 (min^{-1})	0.27	0.39	0.44
	R^2	0.9802	0.9772	0.9807
Pseudo-second-order	Q_e^b ($mg•g^{-1}$)	45.48	47.16	47.73
	K_2 (min^{-1})	0.0093	0.014	0.016
	R^2	0.9996	0.9996	0.9998

Table S5. Fitting parameters for the Langmuir and Freundlich model that describe Cd(II) adsorption on FeS_2@P^{bm} at 298 K.

Model	Parameter	Temperature (298 K)
Langmuir	Q_m (g•g^{-1})	54.83
	k_L (L•g^{-1})	0.60
	R^2	0.9936
Freundlich	1/n	0.13
	K_F (mg•g^{-1}(L•min^{-1})1/n)	32.75
	R^2	0.9759

Table S6. Comparison of the maximum adsorption capacity for Cd(II) by various adsorbents as reported in literature.

Adsorbent	Isotherm model	Solution pH	Adsorbent dosage ($g \cdot L^{-1}$)	Adsorption capacity ($mg \cdot g^{-1}$)	Reference
MBC ($MgCl_2$ modified BC)	Langmuir	5	1	763.12	[1]
pine bark	Freundlich	5	9.2	7.5	[2]
STB (sludge-tire composite biochar)	Langumuir	7	5	50.25	[3]
Aqueous solution by phosphogypsum	Freundlich	9-11	10	131.58	[4]
Jordanian natural zeolite	Freundlich	6	5	25.9	[5]
Natural limestone	Freundlich	5	25	8.87	[6]
CM400 (earthworm manure)	langumuir	5.5	2	24	[7]
$FeS_2@P^{bm}$	Freundlich	5.8	0.4	54.83	This work

Reference

[1] G. Yin, L. Tao, X. Chen, N. S. Bolan, B. Sarkar, Q. Lin, H. Wang, *J. Hazard. Mater.* 2021, **420**, 126487. https://doi.org/10.1016/j.jhazmat.2021.126487

[2] S. Al-Asheh, Z. Duvnjak, *J. Hazard. Mater.* 1997, **56**，35-51. https://doi.org/10.1016/s0304-3894(97)00040-x

[3] X. Fan, J. Zhang, Y. Xie, D. Xu, Y. Liu, J. Liu, J. Hou, *J. Water. Sci. Technol.* 2021, **83**, 1429-1445. https://doi.org/10.2166/wst.2021.058

[4] B. Nilgün, C. Hasan, *Chem. Eng. J.* 2008*,* **140.** 247-254. https://doi.org/10.1016/j.cej.2007.10.002

[5] M. Allawzi, S. Al-Asheh. *Desalin. Water. Treat.* 2010, **22**, 349-354. https://doi.org/10.5004/dwt.2010.1200

[6] B. Knežević, V. Kastratović, *Ecol. Chem. Eng. S.* 2025, **32**, 367-386. https://doi.org/10.2478/eces-2025-0018

[7] Z. Wang, D. Shen, F. Shen, C. Wu, S. Gu, *J. Mol. Liq.* 2017, **241**, 612-621. https://doi.org/10.1016/j.molliq.2017.05.097